RSC Advances

RSC Publishing

COMMUNICATION

View Article Online
View Journal | View Issue

Rapid, microwave-assisted synthesis of battery-grade lithium titanate (LTO)†

Cite this: *RSC Advances*, 2013, **3**, 15618

Received 30th April 2013,
Accepted 9th July 2013

DOI: 10.1039/c3ra43237h

www.rsc.org/advances

Lea V. Nowack,[a] Oliver Waser,[b] Olesya Yarema[a] and Vanessa Wood*[a]

We report a fast, scalable, and low energy approach to synthesize battery-grade $Li_4Ti_5O_{12}$ (LTO). Low-temperature, microwave-assisted solvothermal synthesis yields nanoplatelets that self-assemble into microspheres. Following calcination, these microspheres exhibit capacities of 170 mAh g^{-1} and a capacity retention of 99% over 100 cycles.

Rechargeable lithium ion batteries are not only widely used as energy storage for portable devices,[1] but are also poised to play an important role in the rapidly growing markets of electric mobility and grid integration of renewables. Adopting new active materials is an important step to achieve higher energy density, longer lifetimes, and increased safety. However, many of the proposed new materials are cost prohibitive, which highlights the need for low cost, high throughput manufacturing approaches.[2,3]

For example, spinel LTO is a promising candidate to replace graphite as negative electrode material due to its safety and long cycle life. Compared to graphite, LTO has a high potential plateau of 1.55 V *vs.* Li/Li^+, limiting the formation of a solid-electrolyte interface (SEI) and the accompanying risk of gas evolution or decrease in Coulombic efficiency.[4,5] Furthermore, the LTO crystal lattice experiences no strain-induced stress during lithium ion-insertion, leading to an estimated calendar life of more than 20 years.[6] Finally, lithium ion insertion is guaranteed even at high rates, suppressing dangerous electroplating of lithium on the electrode surface at the end of high-rate lithiation. Despite the reduced energy density due to the high lithium ion-insertion voltage, LTO is attractive for vehicle applications since its inherent safety and fast lithium ion-insertion kinetics. These features are considered key for electrical vehicle applications.[7,8]

To date, however, LTO is produced primarily through energy and time intensive processes (>12 h) at high temperatures (>800 °C). These approaches include solid state reaction synthesis[9–13] and soft chemistry routes (*e.g.* sol–gel[14–17] and hydrothermal[18,19]) followed by high temperature annealing as well as combustion methods such as flame spray pyrolysis.[20] Recently, nanosized LTO particles were obtained in less than one minute using supercritical hydrothermal synthesis, but the particles exhibited high internal strains before annealing and therefore low initial capacities.[21] A rapid, low energy synthesis route for LTO with precise control over size and structure is needed.

Most chemical synthesis routes involve conductive heating, where an external heat source transfers energy through the system. The rate of this heat transfer depends on the thermal conductivities of the various materials that must be penetrated. This introduces temperature gradients in the reaction vessel, impeding fast, thermal equilibration. Microwave irradiation, on the other hand, produces efficient internal heating through direct coupling with the molecules and ions in the reaction mixture. Microwave wet chemistry not only reduces the chemical reaction times by several orders of magnitude, but also offers high reaction yields and reproducibility of synthesis protocols due to the suppression of uncontrolled side reactions.[22,23] Since the process does not depend upon thermal conductivity of the materials involved, an instantaneous, simultaneous and uniform rise in system temperature is achieved. Furthermore, when the microwave energy is turned off, only latent heat remains, allowing faster cooling rates.[24,25] This temperature control allows fabrication of highly crystalline and uniformly shaped nanoparticles. While the microwave reactor used in this study (a Discover SP from CEM) produces relatively small amounts of material (in average 200 mg per synthesis), batch-type microwave reactors with volumes up to 12 L as well as continuous flow microwave reactors have been developed, highlighting the scalability of this approach to industrial needs.[26]

Solvothermal microwave-assisted synthesis has already been used to develop lithium ion battery cathode materials, such as lithium iron phosphate.[27,28] Dense layers of LTO were obtained by a dry chemistry synthesis route in a microwave reactor.[29]

Here we present a novel, rapid and low temperature synthesis protocol to achieve battery grade LTO microspheres, which exhibit

[a]*ETH Zurich, Gloriastrasse 35, 8092 Zurich, Switzerland. E-mail: vwood@ethz.ch; Fax: +41 44632 1194; Tel: +41 44632 5913*

[b]*ETH Zurich, Soneggstrasse 3, Zurich, Switzerland. E-mail: oliver.waser@ptl.mavt.ethz.ch; Tel: +41 44632 0943*

† Electronic supplementary information (ESI) available: Particle size distribution, experimental information, results of pristine material. See DOI: 10.1039/c3ra43237h

specific charges close to the theoretical limit and excellent cycling stability.

Metallic lithium is dissolved in benzyl alcohol at 55 °C overnight under argon atmosphere. Titanium(IV) isopropoxide is added to this mixture until a ratio of lithium to titanium of 0.8 is reached. This precursor solution is transferred to a 10 mL glass vial, which is sealed and placed in the microwave reactor. The reaction temperature of 260 °C is achieved in less than two minutes, facilitated by the high ion concentration in the solution. The solution is kept at this temperature for four hours under constant stirring, resulting in high synthetic yields of 91%. As described in the following paragraphs, a calcination step of one hour at 750 °C is introduced in order to obtain highly crystalline LTO. This protocol represents an 80% energy savings compared to a classically heated solvothermal synthesis using an oven-heated autoclave at 250 °C for 48 h.[30] Details of the synthetic yield and energy savings calculations are given in the ESI.†

First we examine the as-prepared material from the microwave reaction prior to calcination. The scanning electron microscopy (SEM) image in Fig. 1a reveals nanoplatelets, loosely assembled into spherical, micron-sized secondary structures. In order to investigate the primary particles by transmission electron microscopy (TEM), we ultrasonicate the microspheres in ispropanol for 5 min. The TEM image in Fig. 1b shows uniform nanoplatelets approximately 7 nm in diameter.

X-ray diffraction (XRD) of the as-prepared material (Fig. 2a) confirms the nanoplatelet shape and size by calculating the crystallite sizes of the three major peaks (hkl = 400, 440, and 111) according to the Scherrer relation. This indicates that the particles contain crystals of nanoplatelet shape with long axis dimensions of 7.3 nm (400) and 5 nm (440), and a thickness of 2.5 nm (111).

Because the XRD data of the as-prepared material shows significant impurities, which, as expected, result in poor electrochemical performance (see ESI†), we introduce a 1 h calcination step, carried out at 750 °C in air in a rotating tube furnace (Carbolite HTR). The XRD data (Fig. 2b) reveals highly crystalline spinel $Li_4Ti_5O_{12}$ with only minor anatase and rutile impurities (7 and 3%, respectively).

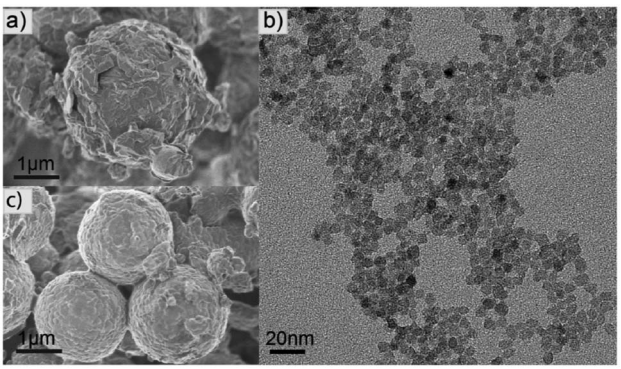

Fig. 1 (a) SEM image of the microwave synthesis product. (b) TEM image of the material shown in (a) after ultrasonification. (c) SEM image of the LTO microspheres after calcination in air at 750 °C.

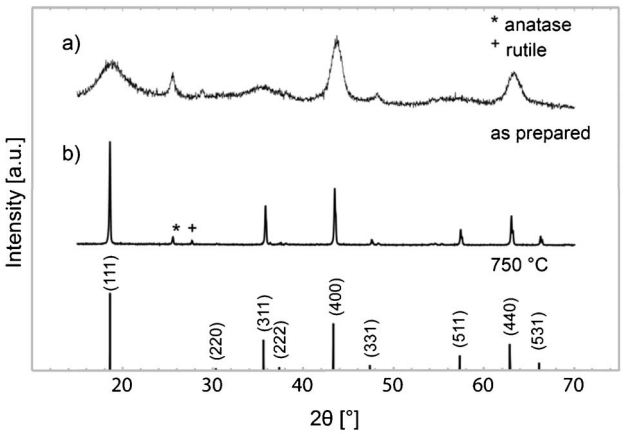

Fig. 2 XRD scans taken with Cu-Kα radiation of the (a) as-prepared and (b) calcined LTO, compared to reference data (ICSD 015787) (bottom). Minor rutile (+) and anatase (*) impurities in the calcined sample are indicated by symbols above the peaks in what is otherwise a highly crystalline LTO material.

We note that, in contrast to other synthesis routes, where introducing excess lithium in the precursor solution often improves phase purity, increasing the lithium concentration here resulted in an as-prepared materials with a large fraction of Li_2TiO_3 impurity, which also has a negative impact on electrochemical performance (See ESI†).

A SEM image of the calcined material (Fig. 1c) shows that the spherical micron-sized particles of the secondary structure are preserved. We further note that groups of 3 to 4 microspheres fused together during calcination, resulting in a particle size distribution with an average particle size of 4.4 μm (see ESI†). Consistent with this observation, XRD data (Fig. 2b) shows that the crystallite size is 150 nm, indicating that the nanoplatelets that were previously loosely assembled into the microsphere have sintered together.

To test the electrochemical performance of our material, we fabricate porous electrodes containing 80 wt% LTO, 10 wt% carbon black (Super P from TIMCAL SA) and 10 wt% polymeric binder (PVDF SOLEF 5130 from Solvay) on an aluminium foil current collector. The electrodes are calendered to reduce the thickness from 84 μm to 56 μm and punched to 13 mm diameter disks. Electrochemical coin type cells are assembled under argon atmosphere using lithium as counter electrode. A fiber-glass separator is soaked with standard organic electrolyte containing 1.0 M $LiPF_6$ in ethylene carbonate (EC) and dimetyhl carbonate (DMC) (1 : 1 by volume).

The test cells are cycled between 1.1 V and 2.4 V *vs.* Li/Li^+ using a constant current/constant voltage procedure. Discharge/charge voltage profiles at room temperature (Fig. 3a), exhibit flat plateaus at 1.55–1.57 V corresponding to reversible insertion of lithium ions to transform $Li_4Ti_5O_{12}$ to $Li_7Ti_5O_{12}$.[31] While the anatase phase of TiO_2 is electrochemically active, the rutile phase is considered inactive. Small influences of the anatase impurities are detected in the slope at the beginning of the voltage curve.

As shown in Fig. 3b, electrochemical measurements are performed at specific currents of 0.1 C–10 C (where 1 C

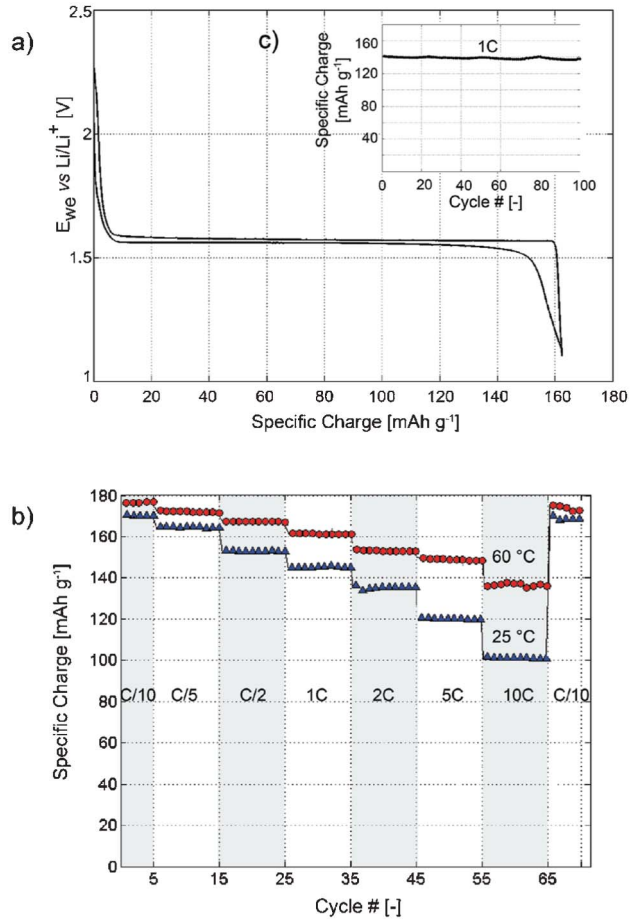

Fig. 3 (a) Specific charge *vs.* E_{we} of a LTO/lithium half-cell cycled galvanostatically at 0.1 C, exhibiting a flat plateau at 1.55 V indicating reversible insertion of lithium ions. (b) Specific charge dependence of the C-rate for the same cell at room temperature (blue) and to 60 °C (red). (c) Specific charge for 100 cycles at a 1 C rate at room temperature demonstrate cycling stability.

corresponds to 175 mA g^{-1}). The room temperature specific charge at 0.1 C is 170 mAh g^{-1}, which is within 97% of the theoretical value of 175 mAh g^{-1}. As expected, at faster cycling rates, the specific charge drops; nevertheless, at 10 C, it is still within 57% of the 0.1 C specific charge, which is comparable to the performance of commercial LTO. Coulombic efficiency is provided in the ESI.†

In order to test whether this drop in specific charge can be explained by slow lithium ion diffusion within the dense LTO microspheres, the cells are again cycled at 60 °C. As shown in Fig. 3b, the theoretical specific charge is reached at 0.1 C and drops only by 20% to 140 mAh g^{-1} at 10 C rates. The improved electrochemical performance at 60 °C, especially for high rates, validates our assumption that the diffusion kinetics at room temperature are rate limiting. Furthermore, this high temperature cycling demonstrates the stability of our material at elevated temperatures.

Fig. 3c highlights the excellent room temperature cycling stability of an annealed microwave-made LTO electrode at 1 C, preserving 99% of its initial specific charge after the 100th cycle (170 mAh g^{-1}) at 0.1 C.

Conclusion

In summary, LTO microspheres consisting of nanoplatelets are obtained by a fast, microwave-assisted solvothermal synthesis. Annealing of samples resulted in highly crystalline LTO, exhibiting high charge/discharge capacities and excellent cycling stability. This represents a reduction in synthesis time from days to hours, and, even by conservative estimates, energy savings of more than 80%.

Microwave-assisted solvothermal synthesis is thus a promising synthesis approach for electrochemically active materials. The ability to synthesize nanoparticles that then self-assemble into micro-sized structures opens the possibility to control, through the introduction of additives, the shape and the porosity of the secondary structures for enhanced high rate cycling performance even at room temperature.

Acknowledgements

This work was supported by the Swiss National Foundation NFP 64. TEM was performed at the Electron Microscopy Facility ETH Zurich. The authors would like to thank Prof. M. Niederberger and Dr I. Bilecka (ETH Zurich) for use of equipment for initial experiments, Prof. Pratsinis (ETH Zurich) for use of XRD and Prof. David Norris for the access to SEM.

Notes and references

1 J. B. Goodenough and Y. Kim, *Chem. Mater.*, 2010, **22**, 587–603.
2 J. M. Tarascon and M. Armand, *Nature*, 2001, **414**, 359–367.
3 D. Doughty and E. P. Roth, *Electrochem. Soc. Interface*, 2012, 37–44.
4 T. Ohzuku, A. Ueda and N. Yamamoto, *J. Electrochem. Soc.*, 1995, **142**, 1431–1435.
5 A. S. Arico, P. Bruce, B. Scrosati, J.-M. Tarascon and W. van Schalkwijk, *Nat. Mater.*, 2005, **4**, 366–377.
6 K. M. Colbow, J. R. Dahn and R. R. Haering, *J. Power Sources*, 1989, **26**, 397–402.
7 V. Manev, *28th International Battery Seminar and Exhibit*, 2011, **1**, 866–882.
8 T. Ohzuku and R. J. Brodd, *J. Power Sources*, 2007, **174**, 449–456.
9 A. Guerfi, P. Charest, K. Knoshita, M. Perrier and K. Zaghib, *J. Power Sources*, 2004, **126**, 163–168.
10 G. G. Amatucci, F. Badway, A. du Pasquier and T. Zheng, *J. Electrochem. Soc.*, 2001, **148**, A930–A939.
11 E. Ferg, R. J. Gummov, A. Kock and M. M. Thackeray, *J. Electrochem. Soc.*, 1994, **141**, L147–L150.
12 K. Zaghib, M. Armand and M. Gauthier, *J. Electrochem. Soc.*, 1998, **145**, 3135–3140.
13 K. Zaghib, M. Simoneau, M. Armand and M. Gauthier, *J. Power Sources*, 1999, **81**, 300–305.
14 C. Shen, X. Zhang, Y. Zhou and H. Li, *Mater. Chem. Phys.*, 2002, **78**, 437–441.
15 L. Kavan and M. Gratzel, *Electrochem. Solid-State Lett.*, 2002, **5**, A39–A42.

16 N. He, B. Wang and J. Huang, *J. Solid State Electrochem.*, 2010, **14**, 1241–1246.
17 D. Shao, J. He, Y. Luo, W. Liu, X. Yu and Y. Fang, *J. Solid State Electrochem.*, 2012, **16**, 2047–2053.
18 K. Nakahara, R. Nakajima, T. Matsushima and H. Majima, *J. Power Sources*, 2003, **117**, 131–136.
19 Y. Lan, X. P. Gao, H. Y. Zhu, Z. F. Zheng, T. Y. Yan, F. Wu, S. P. Ringer and D. Y. Song, *Adv. Funct. Mater.*, 2005, **15**, 1310–1318.
20 F. O. Ernst, H. K. Kammler, A. Roessler, S. E. Pratsinis, W. J. Stark, J. Ufheil and P. Novák, *Mater. Chem. Phys.*, 2007, **101**, 372–378.
21 A. Laumann, M. Bremholm, P. Hald, M. Holzapfel, K. T. Fehr and B. Brummerstedt Iversend, *J. Electrochem. Soc.*, 2012, **159**, A166–A171.
22 M. Larhed and A. Hallberg, *Drug Discovery Today*, 2001, **6**, 406–416.
23 F. Langa, P. Cruz and A. Hoz, *Contemp. Org. Synth.*, 1997, **1**, 373–386.
24 I. Bilecka and M. Niederberger, *Nanoscale*, 2010, **2**, 1358–1374.
25 B. L. Hayes, CEM publishing, Matthews, 2002.
26 J. R. Schmink, C. M. Kormos, W. G. Devine and N. E. Leadbeater, *Org. Process Res. Dev.*, 2010, **14**, 205–214.
27 I. Bilecka, A. Hintennach, M. D. Rossell, D. Xie, P. Novák and M. Niederberger, *J. Mater. Chem.*, 2011, **21**, 5881–5890.
28 A. V. Murugan, T. Muraliganth and A. Manthiram, *J. Phys. Chem. C*, 2008, **112**, 14665–14671.
29 L. H. Yang, C. Dong and J. Guo, *J. Power Sources*, 2008, **175**, 575–580.
30 S.-H. Yu, A. Pucci, T. Herntrich, M.-G. Willinger, S.-H. Baek, Y.-E. Sung and N. Pinna, *J. Mater. Chem.*, 2011, **21**, 806–810.
31 R. A. Huggins, *Advanced Batteries*, Springer, 2009.